

Melting behaviour of poly(phenylene sulphide): 1. Single-stage melt crystallization

Jerry Sengshiu Chung* and Peggy Cebe†

Department of Materials Science and Engineering, Massachusetts Institute of Technology, Cambridge, MA 02139, USA

(Received 20 May 1991; accepted 15 July 1991)

We have studied the melting behaviour of poly(phenylene sulphide), PPS, that has been crystallized from the melt over a wide range of undercooling conditions. Two grades of PPS were used in the study: low molecular weight Ryton V-1 and an experimental medium molecular weight film grade. In this work we report the melting behaviour after a single stage of isothermal melt crystallization. In nearly all cases, dual or triple melting endotherms are seen, but the location and shape of the uppermost endotherm depend upon the degree of undercooling from the melt and on the prior thermal history. At a low degree of undercooling, for both materials, dual endotherms are observed and both melting points increase with the crystallization temperature. Using the immediate rescan technique, we show that the dual endotherms exist together very early in the crystallization process, when only a small fraction of crystals have formed. These results suggest that multiple crystal perfections form early on in the crystallization at low undercooling. As the degree of undercooling increases, the melting point of the uppermost endotherm becomes independent of the crystallization temperature. This result, and the appearance of a triple endothermic response for Ryton at the highest undercooling, indicate that now reorganization of imperfect crystals is dominating the observed endothermic response. We present a model in which the distribution of crystal perfections created during melt crystallization controls the multiple melting behaviour of PPS. At low undercooling conditions, a bimodal distribution of crystals can form which eventually may become two morphologies. At high undercooling conditions, a broad distribution of crystals can form, a part of which may melt and reorganize during the normal d.s.c. scan.

(Keywords: poly(phenylene sulphide); melt crystallization; melting behaviour)

INTRODUCTION

Melting behaviours of various melt crystallized semicrystalline polymers have been studied extensively. This includes polyolefin¹⁻³, nylon⁴⁻⁸, poly(ethylene terephthalate)⁹⁻¹¹, polypropylene¹²⁻¹⁵, poly(etheretherketone)¹⁶⁻²⁵, polystyrene^{26,27} and polyester copolymers²⁸. One very important similarity exists in the melting behaviours of these semicrystalline polymers: multiple melting peaks have nearly always been observed during normal d.s.c. scanning (i.e. at scan rates within the range 5 to 20°C min⁻¹).

The multiple melting behaviour during normal d.s.c. scanning is seen in almost every semicrystalline polymer, in addition to copolymers and blends, that have been crystallized either from the melt or from the rubbery amorphous state. Several models have been proposed in order to explain the multiple melting phenomenon. One model is based on reorganization and another on the existence of several morphologies. By studying fibre materials, such as nylon 66 and poly(ethylene terephthalate), double melting endotherms from both isothermally crystallized and drawn samples have been interpreted to result from the conversion of kinetically favoured lamellar crystals (lower melting point) to

thermodynamically stable extended-chain crystals (higher melting point)^{4-6,11}. However, later investigations^{9,29} showed that this behaviour can be explained by the reorganization of less perfect crystals during the d.s.c. scan.

Several experimental techniques have been used, such as irradiation crosslinking³⁰⁻³², zero entropy displacement^{33,34} and zero scanning rate^{35,36}, to support the view that multiple melting endotherms are attributable to reorganization during the d.s.c. scan. By studying the effect of irradiation on crystallized samples^{30,31}, which prevents reorganization by crosslinking in the amorphous phase, the multiple melting behaviour was seen to disappear and the melting endotherm shifted to a lower temperature. Wunderlich *et al.* developed a very fast d.s.c. scan rate^{33,34} and a zero scan rate^{35,36} technique. They believed the real melting point of the polymer crystals can only be determined under a zero entropy condition³³, and in order to reach the zero entropy condition, the d.s.c. sample must be scanned at a very fast scan rate. They also reported the true melting point of reorganized crystals can be determined by using a zero scan rate technique³⁵.

An alternative view, based on TEM observation of melt crystallized films, is that multiple morphologies are the cause of the multiple endothermic response. In their study of crystal morphology of melt crystallized polyethylene, Bassett *et al.*³⁷ and Bassett and Hodge³⁸

* Present address: Allied Signal Corp., Eng. Plastics, Morristown, NJ 07962, USA

† To whom correspondence should be addressed

suggested that the existence of four endotherms seen in PE melt crystallized at 150°C is correlated to the four types of lamellar crystals of PE. Recently Bassett's group also reported²⁵ that morphology studies of melt crystallized poly(etheretherketone) revealed two distinct kinds of morphologies which consist of dominant lamellae and subsidiary lamellae in samples which exhibited dual endotherms. The dominant lamellae, which may be formed at the early stage of crystallization, will melt at the upper melting temperature. The subsidiary lamellae formed possibly at the later stage of crystallization, which crystallized and infilled between the dominant lamellae, have a lower melting point. Cheng *et al.*²² and Cebe and Chung³⁹ also reported the possible existence of multiple morphologies that may be related to the multiple melting endotherms of semi-flexible polymers like poly(phenylene sulphide) and poly(etheretherketone).

The purpose of this study, which is presented in two parts, is to investigate the cause of the multiple melting behaviour of PPS melt crystallized over a wide range of undercooling. The techniques used in the first part of this study include single-stage isothermal crystallization, immediate rescanning after melt crystallization for various times and the effect of seed crystals generated at high temperatures. The second part of the study⁴⁰ treats the melting behaviour after multiple stages of heat treatment. We find that the multiple melting behaviour, and the dependence of melting temperature on the crystallization temperature, cannot be explained solely on the basis of either a reorganization or a morphology based model. Instead, the nature of the endothermic response is determined by the degree of crystal perfection generated during melt crystallization, and this depends strongly on the degree of undercooling. At low undercooling, we suggest that two levels of crystal perfection are formed, and these may become two distinct morphologies as crystallization proceeds. The melting behaviour will be dominated by the bimodal distribution of crystal perfections. However, at very large degrees of undercooling, only a broad distribution of relatively imperfect crystals can be formed, and these will be subject to reorganization during d.s.c. scanning. The melting behaviour will now be dominated by reorganization leading to the crystallization temperature independence of the upper melting peak.

EXPERIMENTAL

Two grades of poly(phenylene sulphide) powder, Ryton V-1 and experimental film grade, were supplied from Phillips Petroleum Company. The commercial Ryton V-1 is a low molecular weight linear chain PPS (M_w about 15000) containing very low molecular weight oligomers. The experimental film grade is a medium molecular weight grade (M_w about 60000) of lightly branched PPS with melt index of 49 g (10 min)⁻¹. Branching is achieved by incorporating tri-functional monomers into the polymer backbone. Both grades of PPS powder were Soxhlet extracted in tetrahydrofuran for at least 24 h to remove the very low molecular weight oligomers.

The annealing and melting behaviour of the melt crystallized poly(phenylene sulphide) was examined using a Perkin-Elmer DSC-4. PPS powders (10–15 mg) were used with an accuracy in mass within 0.02 mg in most of the experiments. The sample size in any set of

experiments was kept as close as possible. During the sample preparation inside the d.s.c. cell, cooling rates of 200°C min⁻¹ or 320°C min⁻¹ were often used to provide fast cooling. However, this cooling rate is only nominal: the real cooling rate of the sample inside the d.s.c. cell may be slower. The melting peak temperatures and the heat of fusion of PPS samples were calibrated by using indium and bismuth standards. A scan rate of 20°C min⁻¹ was used throughout this investigation unless further specified.

The crystallization kinetics of both Ryton V-1 and film grade have been investigated by using an isothermal d.s.c. program. A PPS sample was heated to 310°C (for Ryton V-1) or 320°C (for film grade), held for 3 min, and then quickly cooled at a rate of 200°C min⁻¹ to the isothermal crystallization temperature, where the crystallization exothermic peak can be observed by monitoring the heat flow as a function of time. Due to the limitation of the cooling rate, the study of crystallization kinetics at very low temperatures (in the range of 100°C to 135°C) was performed by using the cold crystallization technique. The quenched amorphous PPS sample was crystallized directly from the rubbery amorphous state.

The isothermal crystallization of PPS specimens from the melt was performed in the d.s.c. cell. The samples were heated at a rate of 200°C min⁻¹ to 310°C for Ryton V-1 and to 320°C for film grade. Samples were held at this temperature for 3 min to remove all of the polymer crystals before cooling down at 200°C min⁻¹ to the crystallization temperature. The samples were held for 60 min before cooling to room temperature at a rate of 320°C min⁻¹. The cooling rates of 200°C min⁻¹ and 320°C min⁻¹ used between the stages only refer to the nominal cooling rate in the d.s.c. cell, and the actual cooling rate of the samples may not be as fast owing to thermal lag during the fast cooling stage.

How the crystallization and melting behaviour of PPS is affected by the existence of crystal seeds has also been investigated. Different amounts of seed crystals can be artificially generated by controlling the residence time at the isothermal crystallization temperature, here chosen to be 255°C. The Ryton V-1 PPS sample was crystallized at 255°C for various times (0 to 120 min) and then cooled at the rate of 200°C min⁻¹. Relatively imperfect crystals can be formed by crystallizing the uncrystallized fraction from fast cooling.

When both Ryton V-1 and film grade PPS are isothermally melt crystallized at 250°C, the fraction of crystals formed during crystallization is determined by the residence time. In order to investigate the melting behaviour of the incompletely crystallized sample, both grades of PPS samples were immediately rescanned, from the crystallization temperature without cooling, after melt crystallization at 250°C for various times. To avoid any melting of the pre-formed crystals before the d.s.c. was stabilized, a slow scan rate of 5°C min⁻¹ was used.

RESULTS

Crystallization kinetics

Plots of t_m versus the crystallization temperature, T_c , of the film grade PPS and Ryton V-1 are shown in Figure 1. Points on the right were obtained from melt crystallization samples and show that the melt crystallization kinetics of both grades of PPS becomes slower as the crystallization temperature increases. Points on

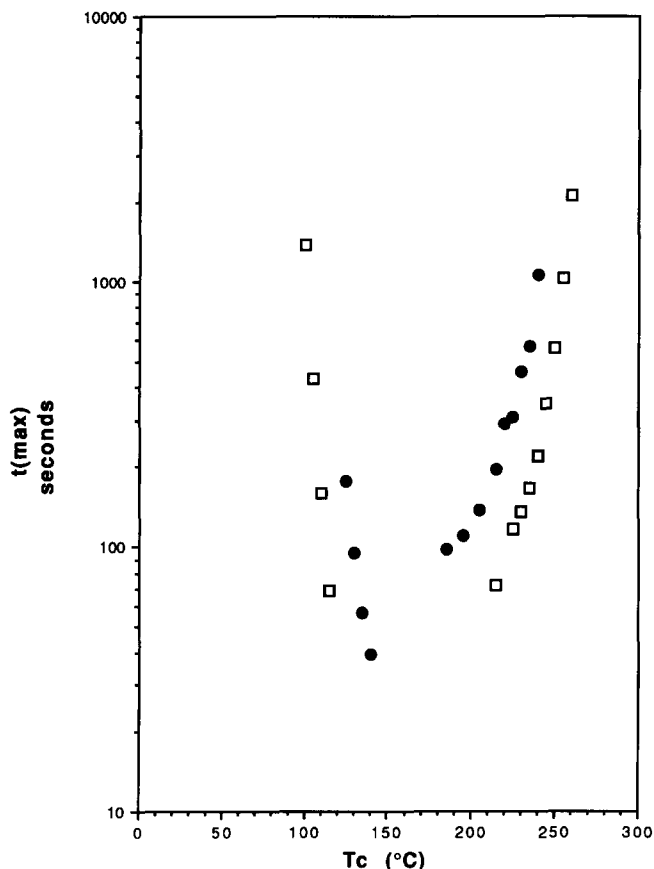


Figure 1 Time required to reach the maximum of the isothermal d.s.c. crystallization exotherm, t_m , versus crystallization temperature, T_c , for Ryton V-1 (\square) and film grade PPS (\bullet)

the left (T_c below 140°C) were obtained by crystallizing quenched amorphous polymer by heating above T_g . These data have been presented previously when the cold crystallization behaviour of PPS was reported⁴¹. The cold crystallization kinetics becomes very rapid as the cold crystallization temperature increases. We were unable to obtain the melt crystallization exotherms at crystallization temperatures below 180°C for film grade, and below 200°C for Ryton V-1, owing both to the limitation on the d.s.c. cooling rate and to the very fast crystallization rate. For the same reason, we could not obtain kinetic data on cold crystallization from amorphous PPS above 150°C for film grade and above 135°C for Ryton V-1.

Because a portion of the crystallization exotherm disappears at the d.s.c. machine stabilization stage at low crystallization temperatures, instead of using $t_{1/2}$ (half-time) we use t_m , the time required to reach the exothermic peak maximum, for the purpose of crystallization kinetics comparison. We observe that the t_m is within the range of 32 s to 1150 s for Ryton V-1 PPS for T_c ranging from 215°C to 265°C , and 90 s to 1000 s for film grade PPS for T_c from 185°C to 245°C . The relative crystallization rate at different crystallization temperatures was compared by the difference of the time (t_m) required to reach the exothermic peak maximum. The longer t_m is, the slower is the crystallization rate.

Melting behaviour of melt crystallized PPS

The collective thermograms of melt crystallized Ryton V-1 and film grade PPS that have been crystallized at various temperatures from the melt for 60 min are shown in Figure 2. The double melting endotherms were

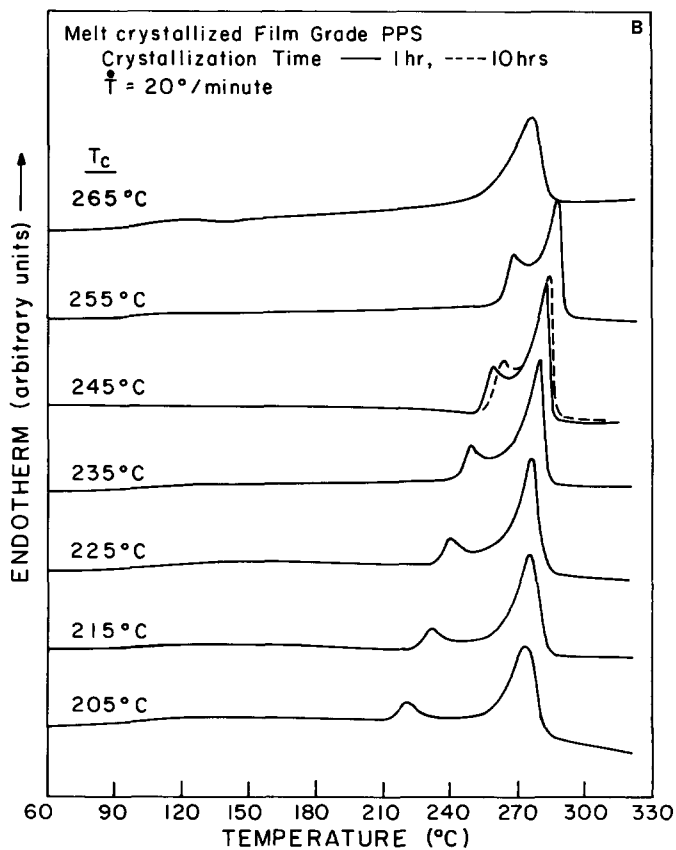
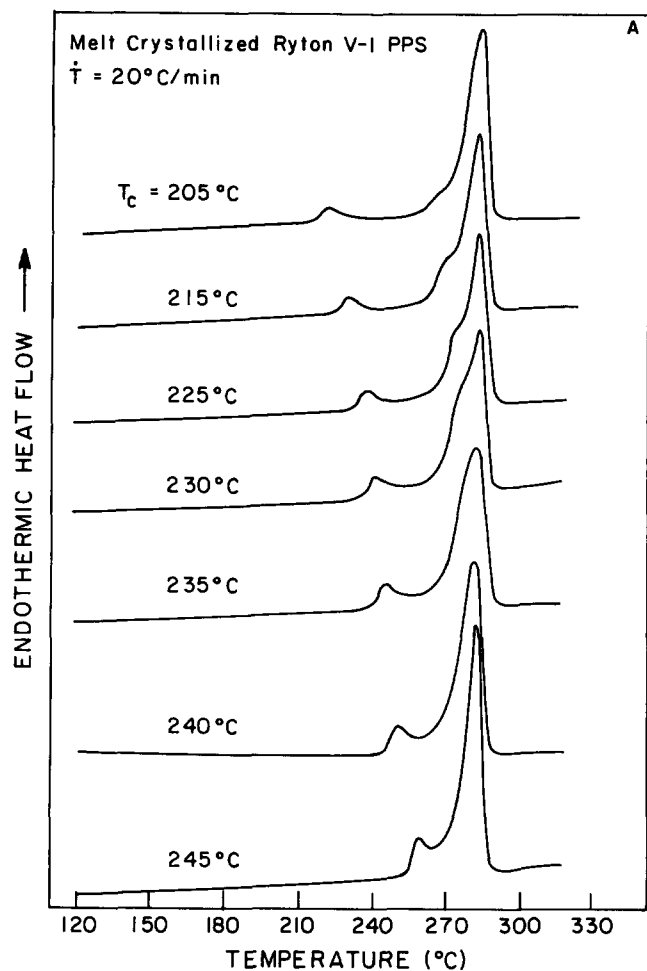


Figure 2 Collective d.s.c. endotherms of PPS melt crystallized at the temperatures indicated for 1 h (solid curves) or 10 h (dashed curve): (A) Ryton V-1; (B) film grade

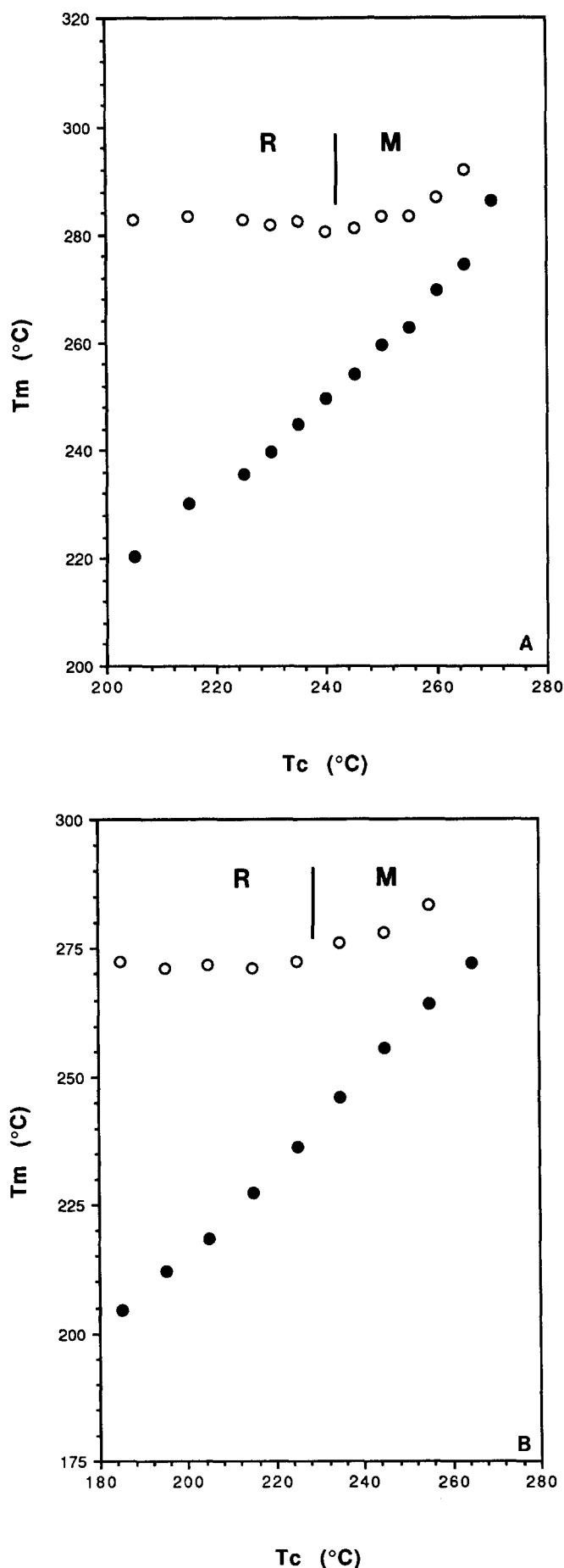


Figure 3 Melting peak temperatures, T_{m1} (●) and T_{m2} (○), versus crystallization temperature for PPS crystallized for 1 h. (A) Ryton V-1; (B) film grade. See text for explanation of the regions designated R and M

observed in most samples when the crystallization temperature was lower than 260°C for film grade and 265°C for Ryton V-1. Careful inspection of the melting endotherm of Ryton V-1 in Figure 2A shows that there is a triple melting peak when the PPS was melt crystallized below 230°C. A third middle peak, T_{m^*} , located in the front shoulder of the upper melting peak was observed at these very large undercooling crystallization conditions. The third middle melting peak shifted to a higher temperature as the crystallization temperature was increased from 205°C to 230°C, finally overlapping with the upper melting peak to form a broad peak. Above 235°C, T_{m^*} cannot be separated.

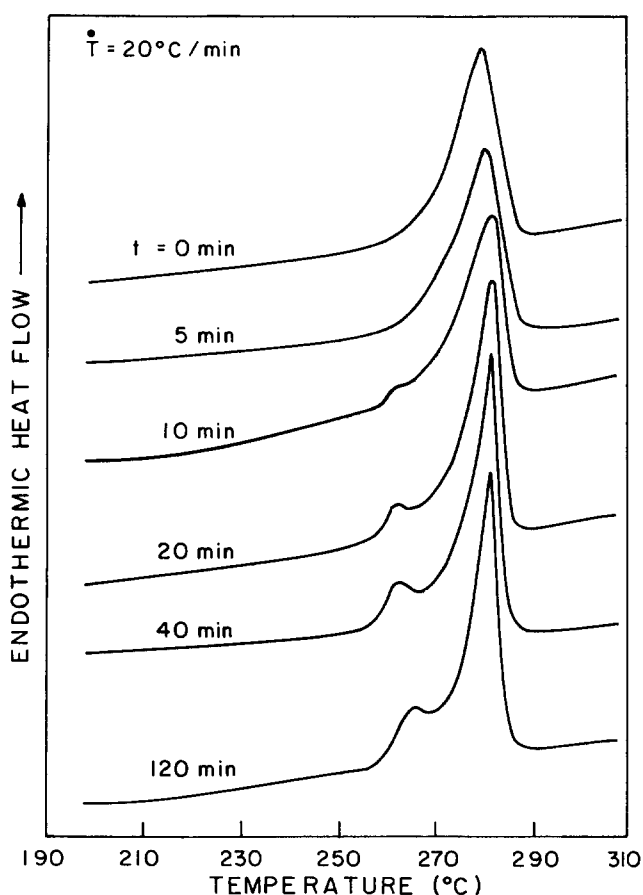
The plots of the upper (T_{m2}) and the lower (T_{m1}) melting peak temperatures of both materials are shown in Figure 3. The T_{m1} s of both materials show an increase with crystallization temperature. However, when the crystallization temperature is lower than 230°C for film grade or 250°C for Ryton V-1, the T_{m2} s remain constant and independent of the crystallization temperature. The T_{m2} s then increase as T_c increases, when T_c is higher than 230°C for film grade or 250°C for Ryton V-1. The vertical mark separates the T_{m2} crystallization temperature dependency into two regions. On the left, T_{m2} is independent of T_c , and we consider this region to be dominated by reorganization (R). On the right, T_{m2} increases with T_c , and we designate this region as morphology dominated (M). The model to describe the melting behaviour will be presented in a later section. The heat of fusion (ΔH_f) of both materials, which refers to the degree of crystallinity, shows only a slight increase with T_c and is listed in Table 1. The infinite crystal melting point was calculated by using the intersection of T_{m1} with the line $T_m = T_c$, and is 335°C for film grade and 305°C for Ryton V-1. These results are in the range suggested in other studies^{22,42}.

Crystal seed effect

The effect of the crystals formed at a higher crystallization temperature on the subsequent crystallization during fast cooling is the main subject of this study. The Ryton V-1 was first crystallized at 255°C from the melt for various times, and this was followed by a very fast cooling rate of 200°C min⁻¹ to room temperature. The amount of the crystals formed at 255°C for the preset time can be determined by the immediate rescan technique (described in the following section). The collective thermograms of the Ryton V-1 showing the seed crystal effect are shown in Figure 4. When Ryton V-1 was cooled very quickly from the melt state, a broad single peak was observed upon subsequent scanning. If the melt resided at 255°C for less than 5 min and then was very quickly cooled, the result of the melting endotherm is exactly the same as that directly cooled from the melt without stopping at 255°C. However, when the residence time at 255°C was longer than 10 min, the subsequent melting endotherm exhibited a small endotherm occurring at a temperature T_{m1} . This lower melting peak became more significant as the residence time at 255°C increased, and the upper melting peak became sharper than that of sample directly cooled from melt. The upper melting peak temperature, T_{m2} , slightly increases with the residence time at 255°C when the melt stays at 255°C less than 10 min, and then no longer varies with time. However, the lower melting peak temperature,

Table 1 Melting peak temperatures, T_{m1} and T_{m2} , and the heat of fusion of Ryton V-1 and film grade PPS melt crystallized at various temperatures for 1 h

Film grade				Ryton V-1			
T_c ($^{\circ}\text{C}$)	T_{m1} ($^{\circ}\text{C}$)	T_{m2} ($^{\circ}\text{C}$)	ΔH (cal g^{-1})	T_c ($^{\circ}\text{C}$)	T_{m1} ($^{\circ}\text{C}$)	T_{m2} ($^{\circ}\text{C}$)	ΔH (cal g^{-1})
185	204.4	272.5	10.1	205	220.5	282.6	12.9
195	212.4	271.0	10.2	215	230.1	283.3	13.0
205	218.3	271.7	11.0	225	235.8	282.7	13.3
215	227.3	271.3	10.7	230	239.8	281.7	13.3
225	236.3	272.4	11.4	235	245.0	282.3	13.6
235	246.0	276.0	11.4	240	249.8	280.5	13.7
245	255.6	278.0	11.6	245	254.1	281.2	13.8
255	264.1	283.3	10.2	250	259.4	283.4	13.8
265	272.2	—	11.8	255	262.8	283.4	14.0
				260	269.6	286.8	13.9
				265	274.6	291.9	13.5
				270	286.4	—	12.1


Figure 4 Collective endotherms of Ryton V-1 PPS melt crystallized at 255 $^{\circ}\text{C}$ for the times indicated, before fast cooling to room temperature

T_{m1} , shifts to a higher temperature as the residence time increases.

Melt crystallization and immediate rescan

In order to explore the crystal formation sequence during melt crystallization, the melting endotherms were obtained by immediately scanning after the sample was melt crystallized at 255 $^{\circ}\text{C}$ for various times. The collective endotherms of the immediate rescan of film grade and Ryton V-1 PPS at 255 $^{\circ}\text{C}$ are shown in Figure 5. The

plots of heat of fusion of both materials versus the crystallization time at 255 $^{\circ}\text{C}$ are shown in Figure 6. When the residence time at 255 $^{\circ}\text{C}$ is not long enough, (under 60 min for film grade or under 2 min for Ryton V-1), only a small fraction of crystal can be formed. The majority of crystallization is complete within 900 min for film grade and 60 min for Ryton V-1 at 255 $^{\circ}\text{C}$. Although only a small amount of crystals can be formed at short times, if the endotherm scale is expanded we find the melting endotherm of the low crystallinity material has a similar shape to the endotherms from the well crystallized sample. The endotherm is composed of a dominant upper melting peak and an insignificant lower melting peak with a broad melting endotherm in between. The lower melting peak can still be seen even when only a very small amount of crystals have formed, and the size of the lower melting peak slightly increases as the crystallization time increases. This result suggests that the double melting endotherm can be formed in a very short time during crystallization.

DISCUSSION

Crystallization kinetics

From the plots of the time at the exotherm maximum, t_m , versus the crystallization temperature, T_c , of both Ryton V-1 and film grade PPS in Figure 1, we see that the t_m of Ryton V-1 is shorter than that of film grade at the same temperature from both cold or melt crystallization. This result indicates that the crystallization kinetics of the low molecular weight Ryton V-1 PPS is faster than that of medium molecular weight branched film grade PPS at the same temperature. A similar result of molecular weight effect on the crystallization kinetics has been reported by Lovinger *et al.*⁴², Lopez and Wilkes⁴³ and Lopez *et al.*⁴⁴. Based on the crystallization kinetics study from linear crystal growth rates and the overall bulk crystallization rate of various molecular weights of PPS, Lopez and Wilkes⁴³ reported that the overall rate of bulk crystallization of different molecular weight PPS can be described by a single Avrami constant with exponent around 3. Jog and Nadkarni⁴⁵ have also reported the crystallization kinetics of low molecular weight Ryton V-1 and 40% glass fibre filled Ryton R-4 PPS. They found the crystallization half-time, measured

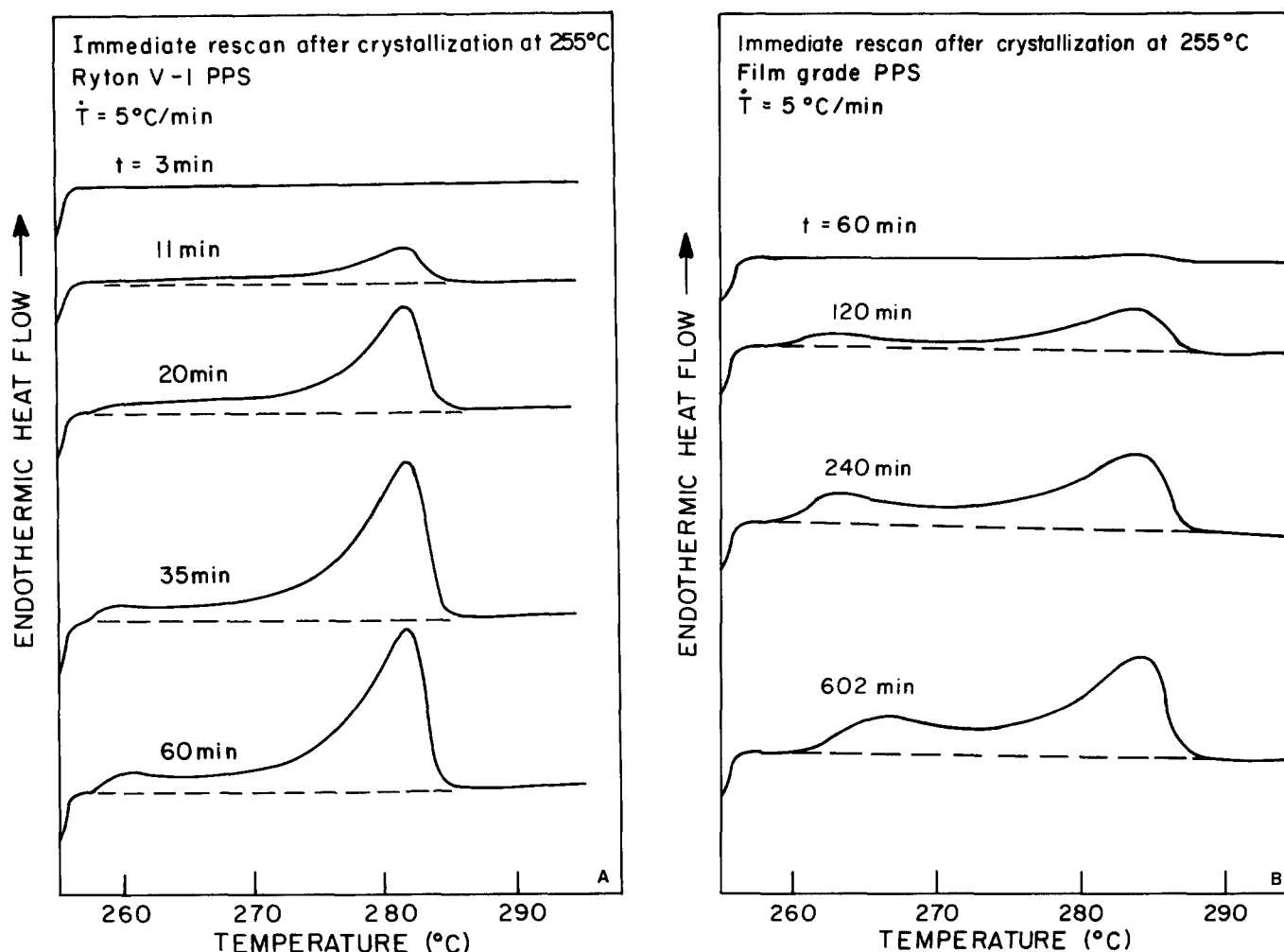


Figure 5 Collective endotherms for PPS scanned immediately after melt crystallization at 255°C for the times indicated: (A) Ryton V-1; (B) film grade

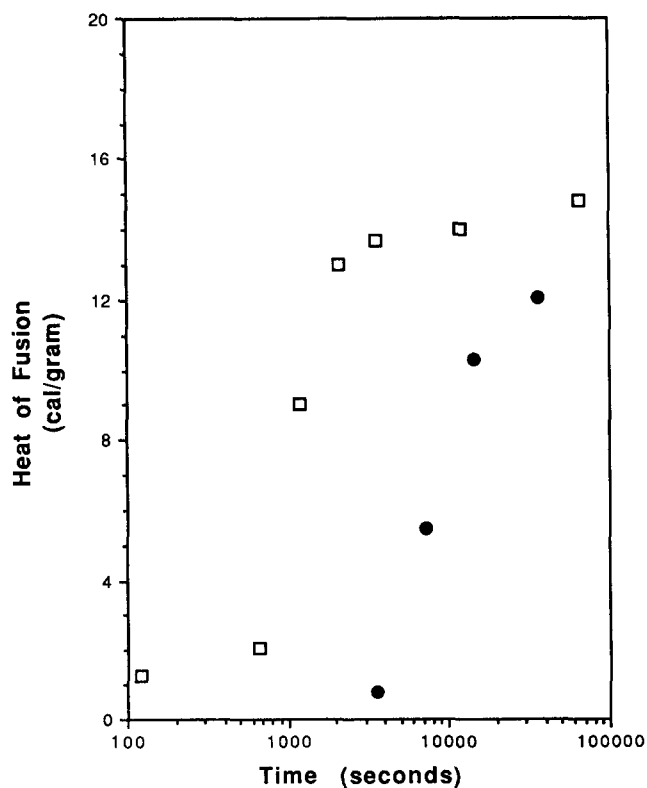


Figure 6 Heat of fusion of PPS versus crystallization time at 255°C, for Ryton V-1 (□) and film grade (●)

from the isothermal d.s.c. endotherm, is 17 to 240 s for Ryton V-1 and 36 to 440 s for Ryton R-4 when the crystallization takes place between 215°C to 250°C. They also reported that the Avrami constant, n , is 2.55 for R-4 and 2.23 for V-1 and does not vary significantly with the crystallization temperature.

Lopez and Wilkes⁴³, Lopez *et al.*⁴⁴ and Jog and Nadkarni⁴⁵ suggested that there exists a simple polynomial relationship between the $t_{1/2}$ s from both melt and cold crystallizations. They assumed that the crystallization kinetics is exactly the same regardless of the initial state (amorphous melt or amorphous solid). This is based on the assumption that the polymer chain conformations before crystallization takes place will be the same regardless of the initial state from either amorphous melt or amorphous solid. However, our kinetic results for the relationship between t_m and T_c of the isothermal crystallization from both melt and rubbery amorphous phases do not fit into a simple polynomial curve. The bulk crystallization kinetics from the rubbery amorphous state apparently is faster than that predicted from the polynomial extrapolation from the melt crystallization. We have already suggested⁴¹ that the existence of the short range ordered structure may be the cause of the unusually fast crystallization kinetics from the rubbery amorphous state.

Although a short range ordered structure can account for the large difference in the bulk crystallization rate, it is unlikely to affect the linear growth rate of an individual

spherulite. Indeed, Lovinger *et al.*⁴² report a smooth transition in the linear growth rate of PPS spherulites grown over a wide range of undercooling conditions. Lovinger and coworkers found that measurements of linear growth rate indicate the existence of a regime II to III transition in the growth behaviour of PPS. There was a range of crystallization temperatures over which the transition occurred, centred at 208°C for the medium molecular weight PPS studied. The endothermic response corresponding to the crystallization temperatures above and below 208°C was not entirely shown. T_{m2} versus T_c was not plotted over the entire crystallization range explored by Lovinger *et al.*⁴², but from the data shown it appears that the regime II to III transition occurs over the range of undercooling at which the crystallization temperature dependency of T_{m2} is changing. At lower undercooling, in regime II of crystal growth, T_{m2} increases linearly with T_c as shown in Figure 3 of ref. 42. At higher undercooling, where Lovinger *et al.* observe regime III growth, the T_{m2} appears to be levelling off, i.e. becoming independent of crystallization temperature. We suggest that the degree of undercooling, which is so important in determining the microscopic characteristics of nucleation and crystal growth, may control the level of bulk crystal perfection (e.g., whether fibrillar or lamellar crystals form, as suggested by Hoffman⁴⁶) and consequently, the bulk endothermic response. Further experiments to compare the regime of crystal growth with the subsequent bulk endothermic response are certainly indicated.

Melting behaviour of PPS

The endothermic response of melt crystallized PPS may consist of one, two or three endotherms depending upon residence time and temperature, after a single stage of melt crystallization. A single endotherm is seen when the time is not long enough for crystals to be generated during the isothermal high temperature stage (Figure 2B, curve 265°C, or Figure 4, $t < 10$ min). In this case a single broad endotherm is seen which represents the melting of crystals formed during cooling. Once crystals form at the isothermal crystallization temperature, dual endotherms are generally seen. However, in Ryton V-1, as the crystallization temperature is decreased, an additional third melting peak is seen to emerge on the low temperature side of the uppermost (T_{m2}) endotherm⁴⁷. The third middle melting peak, T_{m^*} , appears to grow without affecting the peak temperature of T_{m2} . This third endotherm may result from the melting of a more perfect type of crystal present in the material at room temperature, and T_{m1} represents the melting of a less perfect type of crystal, also present in the material at room temperature. T_{m2} would then come from the melting and recrystallization of these two types of crystals during the d.s.c. scan.

Crystal seed effect

From Figure 4, all of the melting endotherms of the Ryton V-1 PPS after various treatment times at 255°C have the same melting range from 253°C to 290°C. The lower melting peak, T_{m1} , can be observed when the residence time at 255°C is longer than 10 min. As the residence time increases, the area underneath the lower melting peak increases, and the peak shifts to a higher peak temperature. The broad upper melting peak becomes much sharper as the residence time increases.

When the residence time is 120 min at 255°C, the full width half maximum of the upper melting peak is about 8°C compared to 15°C for 5 min residence time. The amount of crystals that can be formed at 255°C after various times can be predicted from the study of immediate rescan without cooling (Figure 6). The melting endotherms of the Ryton V-1 crystallized at 255°C for 5 or 10 min indicate that the fraction of crystals formed is only 5% or 10%. The remaining uncrystallized fraction must be subjected to crystallization during cooling at temperatures much lower than 255°C. (We have observed that the nominal cooling rate of 200°C min⁻¹ is not fast enough to quench the Ryton V-1 from the melt to an amorphous state, and crystallization takes place during cooling.) The crystals formed during fast cooling from the melt state should therefore have a melting endotherm at a temperature below 255°C, because the relatively imperfect crystals will be formed at the lower crystallization temperature and will melt at a lower temperature. Then the questions we must address are why the melting

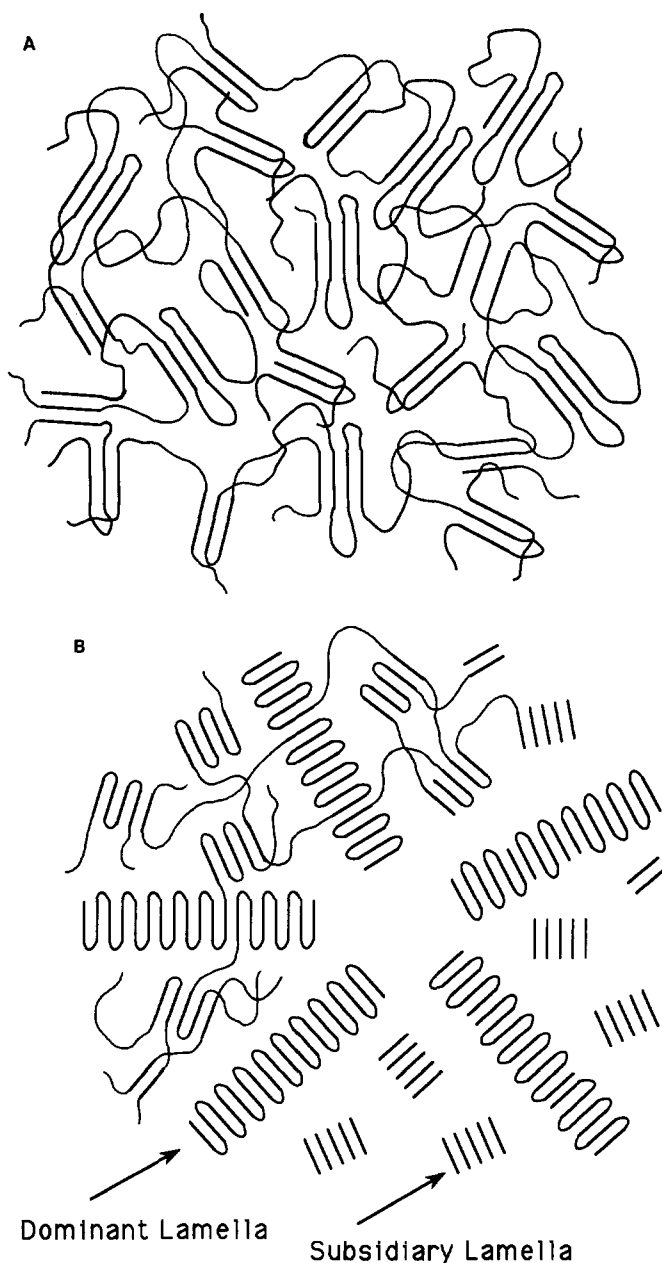


Figure 7 Sketch of proposed morphology of PPS crystallized from the melt at: (A) high undercooling; (B) low undercooling

endotherm of PPS fast cooled from the melt is located above 255°C (*Figure 4*, curve $t = 0$) even when the real crystallization takes place at much lower temperature, and where is the melting endotherm of the fraction uncrystallized at 255°C but which becomes crystallized during fast cooling.

We suggest that the crystals formed during fast cooling are very imperfect, due to very fast crystallization kinetics, and the perfection of the crystals would range over a wide distribution. A sketch of the proposed morphology of crystals formed at high undercooling is shown in *Figure 7A*. Here we depict very imperfect crystals in a highly entangled melt, at low temperature where chain mobility is very low. The actual size distribution of the crystal regions may be very broad, as has been suggested by Bassett *et al.*²⁵. During the d.s.c. scan the imperfect crystals melt and reorganize to form more perfect crystals, and this reorganization process may be happening on a localized scale. The endothermic energy required for the localized melting and the exothermic energy needed for the local reorganization can be compensated for by each other, and hence no net heat flow can be observed as an endothermic maximum from the d.s.c. scan. The wide distribution of crystal perfection of the pre-existing crystals, formed during fast cooling, allows localized reorganization to happen, because melting and reorganization can take place continuously. Therefore, the observed d.s.c. endotherm of the Ryton V-1 crystallized through fast cooling (*Figure 4*, curve $t = 0$) has one broad melting endotherm because the real melting endotherm is completely overlapped with the reorganization exotherm. As the residence time at 255°C increases (*Figure 4*, curves $t = 5-120$), the fraction of the imperfect crystals is reduced and the amount of crystals able to undergo reorganization during the scan is reduced, and therefore the melting distribution of the upper melting peak becomes narrow (see *Figure 4*). Based on this study, we propose that the upper melting peak is related to the melting of a population of crystals which have a more perfect crystal structure. This study supports the view that the very imperfect crystals reorganize during a d.s.c. scan and contribute to broadening of the upper melting endotherm.

Perfection of crystals immediately rescanned without cooling

In the attempt to explore the multiple melting behaviour of the semi-flexible polymers, Bassett *et al.*²⁵ and Cheng *et al.*^{22,48} have investigated the immediate d.s.c. rescan of PEEK and PPS after melt crystallization at an isothermal crystallization temperature for various times. They reported that the upper melting peak is formed at the early stage of crystallization and the lower melting peak formed only after a certain time, such as after a time longer than required for spherulite impingement. They therefore suggested that the double melting behaviour of these semi-flexible polymers is due to two kinds of morphologies formed during isothermal crystallization from the melt. A sketch of the two morphologies that may exist together at high temperature is shown in *Figure 7B*. Dominant lamellae and subsidiary lamellae may coexist in the melt at elevated temperatures where chain mobility is high. Such dual morphologies have already been observed in PEEK²⁵ crystallized at low undercooling. While our results in PPS support a role of morphology in determining the dual endothermic

response at low undercooling, we still find some important differences in our results for the immediate rescan compared to those of Bassett *et al.*²⁵ and Cheng *et al.*^{22,48}.

In the immediately rescanned endotherms reported by Bassett *et al.*²⁵ and Cheng *et al.*⁴⁸ some information appears to be lost at the start of the scan. In our experience, at a scan rate of 20°C min⁻¹ it takes about 20 s for the Perkin-Elmer DSC model 4 to reach stabilization. The scan rates used in the previous investigations are too fast (16°C min⁻¹ and 20°C min⁻¹) and therefore some of the endotherm curve is lost in the machine stabilization stage. We performed the immediate rescan at a heating rate of 5°C min⁻¹ for Ryton V-1 and film grade PPS which had been crystallized at 255°C for various times. The slower heating rate allows us to obtain the entire d.s.c. rescan endotherm without losing any information in the initial stage. This is evidenced by the return to baseline before the endothermic heat flow begins (see *Figure 5*). The percentage of crystals formed, estimated from the heat of fusion of the rescan endotherm (shown in *Figure 6*), is less than 10% when the residence time at 255°C is 60 min for film grade or 3 min for Ryton V-1. However, we found these rescan endotherms do not look like the endotherms shown by Bassett *et al.*²⁵ or Cheng *et al.*^{22,48}. Instead of the single upper melting peak formation at an early stage of the crystallization proposed by these authors, we found the rescan endotherm after short residence time has a very similar shape to that of a completely crystallized sample, when all melting endotherms were enlarged to the same size. Even in the case of the earliest crystallization times reported in *Figure 5* (3 min for Ryton, and 60 min for film grade), although the curves look very featureless on the scale shown, we found no differences in the relative sizes of the endotherms when they were increased to the same size. We found that *double* melting endotherms can be observed in the immediate rescan of both grades of PPS even after very short time at 255°C. The immediate rescan endotherm of both grades of PPS consists of a strong dominant upper melting peak T_{m2} and a broad melting endotherm as a tail in front of the upper melting peak. The lower melting peak T_{m1} is located at the low temperature end of this broad endotherm and has a melting peak temperature about 5° to 10°C higher than the isothermal crystallization temperature.

In an attempt to explain the result for the immediate rescan of PEEK, Blundell and Osborn¹⁶, Blundell¹⁹ and Lee and Porter^{20,21} suggested that the cause of the double melting peak development is due to reorganization. Both groups proposed that the reason the upper melting peak develops at short times is solely reorganization. However, we find the proposed reorganization model cannot be used to explain our result for the immediate rescan. In general, the reorganization rate should be either slower than, or comparable to, the crystallization rate at the same temperature, because of the hindrance effect of the existing crystals and the relatively low chain mobility. The reorganization rate should also behave like the crystallization rate which (as shown in *Figure 1*) is strongly dependent upon the treatment temperature. Therefore a much slower reorganization rate should be expected at a higher temperature. Hence, when PEEK or PPS was melt crystallized at a relatively low degree of undercooling (which was used for most of the immediate rescan studies) the crystallization rate is very

slow due to the relatively high temperatures used. During the immediate rescan of the partially or fully crystallized sample after longer crystallization time, the existing crystals will not be able to proceed to a major structural reorganization, because they will be exposed to much higher temperatures at which the reorganization or recrystallization rate is much slower compared to the heating rate. Hence the double melting behaviour of the immediate rescan of the semi-flexible polymers crystallized at relatively small undercooling conditions should not be due to the reorganization of existing unperfected crystals.

We suggest that the double melting endotherm of PPS is due to two distributions of crystal perfection even at early crystallization times, which eventually become two kinds of crystal morphologies, as suggested for PEEK by Bassett *et al.*²⁵. However, unlike the morphology model suggested by Bassett *et al.*^{25,37} and Bassett and Hodge³⁸, we suggest that these two distributions of crystals are formed at about the same time in PPS, and that both the perfect (controlled by the balance of both thermodynamics and kinetics factors) and imperfect crystals (solely controlled by kinetics factors) may be formed even in the initial stages of crystallization when only 5–10% of crystals have formed. During the crystallization, the relatively imperfect crystals grow in a geometrically constrained region between the lamellar crystals, and two kinds of morphologies are eventually formed: dominant lamellae (more perfect) and subsidiary lamellae (less perfect), as shown in *Figure 7B*. A similar result has been reported for PEEK by Bassett *et al.*²⁵ based on a crystal morphology study.

The melting point of an individual crystal depends on its lamellar thickness, size of the crystal, perfection of molecular packing inside the lattice, and the defect structure and its distribution^{49–53}. Since the crystallization of polymers is a kinetically controlled process, it depends upon the crystallization rate and upon the chain mobility of the polymer chain segments which can attach together and initiate the crystallization. From our results, it appears that any kind of crystal perfection may be formed as long as the melting points are higher than the crystallization temperature. The melting point distribution of the melt crystallized crystals is related to the level of crystal perfection which can be formed during isothermal melt crystallization and will strongly depend upon the crystallization kinetics. Therefore the melting point of crystals formed from the isothermal melt crystallization would be a distribution that covers from a few degrees above the crystallization temperature to a maximum temperature above which all of the crystals melt.

A model for the melting behaviour of melt crystallized PPS

In this section we present a model to describe the differences in distributions of crystal perfection that arise during melt crystallization at small and large undercooling. This model is based on crystallization kinetics considerations, and was developed in order to explain the multiple melting behaviour as well as the dependence of the uppermost endotherm on crystallization temperature: at low undercooling, T_{m2} increases linearly with T_c , while at high undercooling, T_{m2} is independent of T_c . While our description is based on experimental evidence obtained for PPS, we believe the model to be quite

generally applicable to the melting behaviour of high performance polymers that are capable of crystallizing over a wide range of undercooling conditions.

The melting behaviour of a melt crystallized polymer sample must be related to the pre-existing crystal structure and morphology, which are strongly affected by the crystallization kinetics. The crystallization rate of PPS is controlled by factors such as crystallization temperature, molecular weight, chain branching etc. Changing one of these factors will alter the crystallization kinetics; therefore the crystal structure (crystal packing perfection) and morphology will also be altered. The random coils of polymer molecules in the melt state are heavily interpenetrated and entangled with each other. In order to form a more perfect crystal structure, polymer chains require enough mobility and time to disentangle and then pack into lattice crystals to form a folded chain lamella. Unlike the nucleation rate, the polymer chain mobility is higher at a higher temperature, and hence the balance between the nucleation rate and chain mobility will be very important to determine the perfection of the crystal structure. In this study, we report that the dual melting behaviour of the melt crystallized Ryton V-1 and film grade PPS may be due either to reorganization of existing crystals or to melting of two kinds of crystals, depending upon the crystallization conditions. If the PPS were crystallized at a lower crystallization temperature, for example 225°C for Ryton V-1, at which the nucleation rate is very fast and chain mobility is very low, the appearance of dual melting peaks is dominated by reorganization. However, when the PPS was crystallized at a small undercooling condition, for example 255°C for Ryton V-1, at which the nucleation rate is slow but chain mobility is high, the cause of dual melting is the existence of two kinds of crystal perfection as shown in *Figure 7B*.

If the crystallization takes place at a large undercooling condition at which the nucleation rate and subsequent growth are much faster than the chain disentanglement rate, the entangled chains will be unable to relax their entanglement during crystallization, and the perfection of the crystal and the ability to form chain folded lamellar crystals will be restricted by the chain entanglement effect. The resulting crystal perfection has a broad distribution and its crystal structure is relatively imperfect (*Figure 7A*), as also confirmed by wide angle X-ray scattering experiments^{44,51,52,55}. Based on the multiple stage crystallization experiment, which is presented in the second part of the research⁴⁰, we suggest that the real melting point of the imperfect crystals is relatively low. Since the reorganization rate, like the crystallization rate, is relatively high at low temperatures, reorganization will be able to take place very easily after the imperfect crystals melt at the low temperature during a d.s.c. scan. Hence the upper melting endotherm of PPS melt crystallized at very large undercooling contains a large contribution from the melting and then reorganization of the imperfect crystals at the lower temperature, followed by remelting at the higher temperature.

However, if the crystallization takes place at a small undercooling condition, such that the nucleation rate and subsequent crystal growth are much slower than the disentanglement rate, two kinds of crystal populations can be formed. First, from only thermodynamics considerations, the extended chain crystal should have been formed since that minimizes the free energy. But kinetic nucleation factors will favour the formation of the fold

chain crystal. By balancing the thermodynamics and kinetics factors at the crystallization conditions, the folded chain crystal lamellae can be formed through relaxing the entangled chain. These folded lamellar crystals have better crystal perfection and will melt at a higher temperature. Second, based on the crystallization kinetics consideration, any kind of crystals that have a melting point higher than the isothermal crystallization temperature will also be formed. The less perfect crystals may be formed through the kinetically controlled process by attaching polymer chain segments together randomly (more like fringed micellar crystals). The polymer chains have not been disentangled before packing into the crystal lattice and the crystals formed have a relatively imperfect structure. The perfection of these imperfect crystals will have a broad distribution, and the crystals will melt in the range between the isothermal crystallization temperature and the melting temperature of the perfect fold crystals. At just a few degrees higher than the crystallization temperature, the imperfect crystal population is higher and results in a small lower melting peak T_{m1} . Since the formation of these two kinds of crystal are controlled by different factors, both of the crystals, perfect folded chain lamellae and imperfect crystals, can be formed at the initial stage of crystallization. As the crystallization progresses, the folded chain lamellae eventually become the dominant lamellae, and the imperfect crystals, identified as subsidiary lamellae, are then excluded to fill the space in between. Therefore, two kinds of morphologies can be formed at the small undercooling crystallization conditions. Hence the dual melting endotherm of the PPS melt crystallized at the low undercooling condition is due to the melting of these two kinds of crystals.

Our model is based on the crystallization kinetics dependency of crystal morphology. When PPS is melt crystallized at a low crystallization temperature (high degree of undercooling: here larger than 60°C) the size and location of the upper melting endotherm is dominated by the melting of the reorganized crystals. Therefore the upper melting peak temperature is not a function of the crystallization temperature. On the other hand, the upper melting endotherm from PPS melt crystallized at high crystallization temperature (small undercooling: here smaller than 25°C) is due to the melting of pre-existing more perfect folded chain lamellar crystals. Therefore the upper melting peak temperature is proportional to the crystallization temperature because the crystal perfection and the lamellar thickness both increase with crystallization temperature. Based on a consideration of crystallization kinetics, the transition from reorganization regime to the regime dominated by two morphologies should be related to the crystallization rate of PPS. The upper melting peak temperatures of both Ryton V-1 and film grade PPS, which have been melt crystallized at T_c for 60 min, are plotted versus the time required for the exothermic peak maximum from the isothermal crystallization experiment. Results are shown in Figure 8, and indicate that regardless of the large crystallization rate difference between Ryton V-1 and film grade at the same temperature, the transition from reorganization domain to the two-morphology domain is taking place at a similar crystallization rate for both grades of PPS (at which t_m has a value of about 200–300 s).

To test the model, we used the scan rate dependency of the lower and upper melting point temperatures for

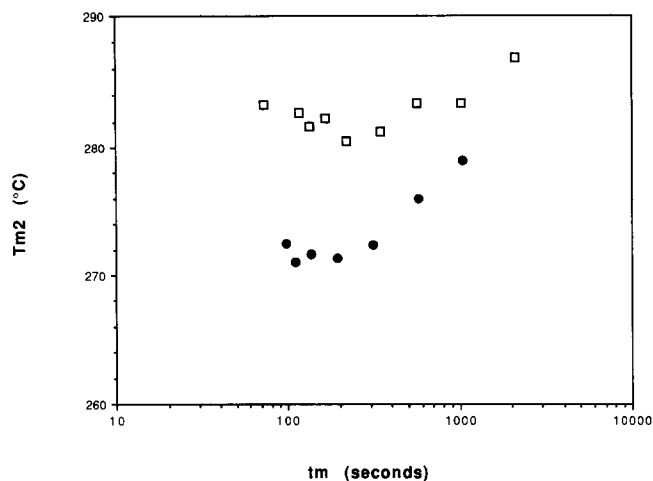


Figure 8 Upper melting peak temperature, T_{m2} , versus t_m , the time to reach the maximum in the isothermal crystallization exotherm, for Ryton V-1 (\square) and film grade (\bullet) PPS

Ryton V-1. We selected three crystallizations which represent the conditions of morphology domination or reorganization. For the former, we chose melt crystallization at 260°C, which according to Figure 3A is in the morphology (M) dominated region. For the latter, we chose melt crystallization at 240°C (larger undercooling, and from Figure 3A just in the reorganization (R) region) and cold crystallization at 250°C. From our previous work reporting the behaviour of cold crystallized PPS⁴¹, we believe that reorganization of imperfect crystals during the scan is controlling the observed dual endothermic behaviour. Thus, our model would imply that the cold crystallized sample should show the same behaviour as a sample melt crystallized at large undercooling.

T_{m2} should have a strong dependence upon the d.s.c. scan rate under conditions dominated by reorganization: T_{m2} would be expected to increase strongly as the scan rate decreases during cold crystallization or during melt crystallization at a large degree of undercooling. On the other hand, if reorganization is not playing a major role in determining the size and shape of the upper endotherm, we anticipate that the upper endothermic peak temperature will not be strongly affected by the scanning rate. This would be the case for melt crystallization at a low degree of undercooling.

Results of scan rate dependence are shown in Figure 9 for the three treatments, with scan rate varying from 1°C min⁻¹ to 60°C min⁻¹. Figures 9A and 9B show the scan rate dependence for the cold crystallized sample ($T_c = 250^\circ\text{C}$) and the highly undercooled melt crystallized sample ($T_c = 240^\circ\text{C}$), respectively. Over the scan rates tested, the upper endotherm temperature increases significantly with decreasing scan rate. T_{m2} for PPS cold crystallized at 250°C increases 9°, and T_{m2} for PPS melt crystallized at 240°C increases 11°, as scan rate decreases from 60 to 1°C min⁻¹. In contrast, T_{m2} for PPS melt crystallized at 260°C (lower undercooling) changes only 3° over the scan rates tested. These results support our idea that reorganization does not play a major role in determining the upper endothermic response of PPS melt crystallized at low degree of undercooling, but reorganization is significant for crystallization at large undercooling, whether from the melt or from the rubbery amorphous state. However, these scan rate tests were

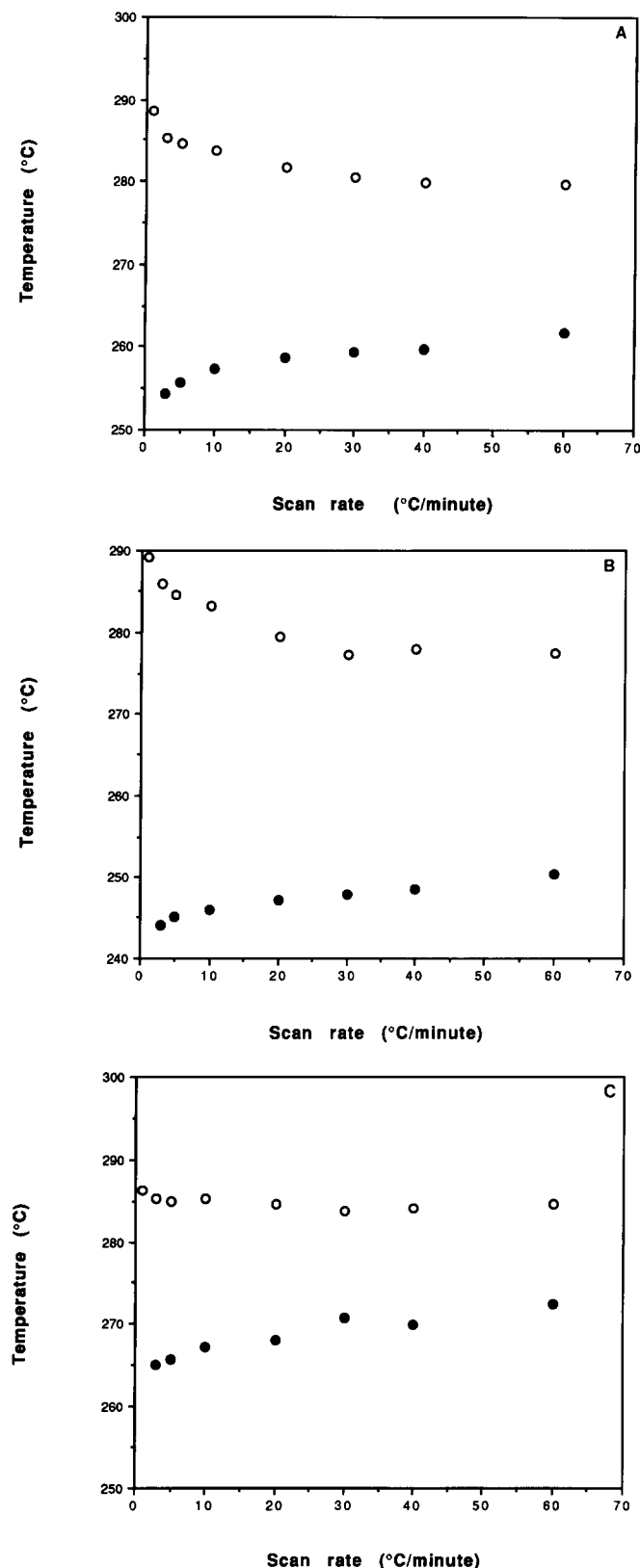


Figure 9 Melting peak temperatures, T_{m1} (●) and T_{m2} (○), versus scan rate for Ryton V-1 PPS crystallized at: (A) 250°C, cold crystallization; (B) 240°C, melt crystallization; and (C) 260°C, melt crystallization

performed for crystallization temperatures near the dividing line between the reorganization region (R, in Figure 3) and the morphology region (M, in Figure 3). Further tests of scan rate dependence are planned at both higher and lower crystallization temperatures.

The original melting endotherm, reorganization exotherm and remelting endotherm of PPS are shown in Figure 10 for melt crystallization at large and small undercooling conditions. In the lower half of each figure the resultant d.s.c. thermogram is shown. In Figure 10A the original crystals are shown to have a very broad distribution of melting points, as suggested by Bassett *et al.*²⁵. The least perfect crystals are subject to reorganization, so a large reorganization exotherm is depicted. The resultant d.s.c. endotherm T_{m2} is shown to contain a significant contribution from reorganization of the imperfect crystals. In this study, and in the second part relating to multiple stage melt crystallization⁴⁰, we were never able completely to eliminate the uppermost endotherm (for example, by fast scanning to reduce the chance for reorganization). Thus, T_{m2} contains a contribution from the pre-existing crystals as suggested by Bassett *et al.*²⁵.

The positioning of the original melting endotherm in Figure 10A is arbitrary, as no information is available about the real shape and position. The resultant thermogram will depend strongly on the location of the maximum in the original melting endotherm, and may account for the differences between Ryton and film grade PPS. In the case of Ryton V-1, triple endotherms are seen for the highest undercooling conditions, whereas for film grade we never observed the triple endotherm after a single stage of isothermal crystallization. Recently, Nichols and Robertson⁵⁶ provided a possible explanation for the triple endothermic behaviour, when a single broad crystal population exists in the sample prior to the d.s.c. scan. These workers showed that it is possible for a single distribution to reorganize so that the low melting tail gives T_{m1} . Crystals near the centre of the distribution melt to give T_{m*} . Then the uppermost melting peak, T_{m2} , is due to reorganization of the imperfect crystals during the d.s.c. scan⁵⁶. We utilized this idea in Figure 10A. However we have additional evidence to be presented in Part 2⁴⁰ that crystals melting to form T_{m*} , may also be subject to reorganization, and may contribute to T_{m2} .

The proposed endotherms, and the resultant d.s.c. thermogram of PPS which has been melt crystallized at a small undercooling are shown in Figure 10B. It shows that the dual melting d.s.c. endotherm is due to two kinds of crystals (with two levels of crystal perfection) which have only a small scale of reorganization. This view is supported by the morphology studies of Bassett *et al.*²⁵ on PEEK in which dual populations of crystals were identified, as shown in the sketch in Figure 7B. Morphology studies of melt and cold crystallized PPS are areas of future research.

CONCLUSION

We have proposed a model based on crystallization kinetics considerations to explain the dual melting behaviour of melt crystallized PPS. When PPS is crystallized at small undercooling, the crystal structure and morphology formed during crystallization may result in the creation of two different levels of crystal perfection, which may develop into two distinct morphologies as crystallization proceeds. The observed multiple melting behaviour is in the morphology domain. The dual melting endotherms found in the d.s.c. scan are due to the melting of the two crystal populations both existing in the sample

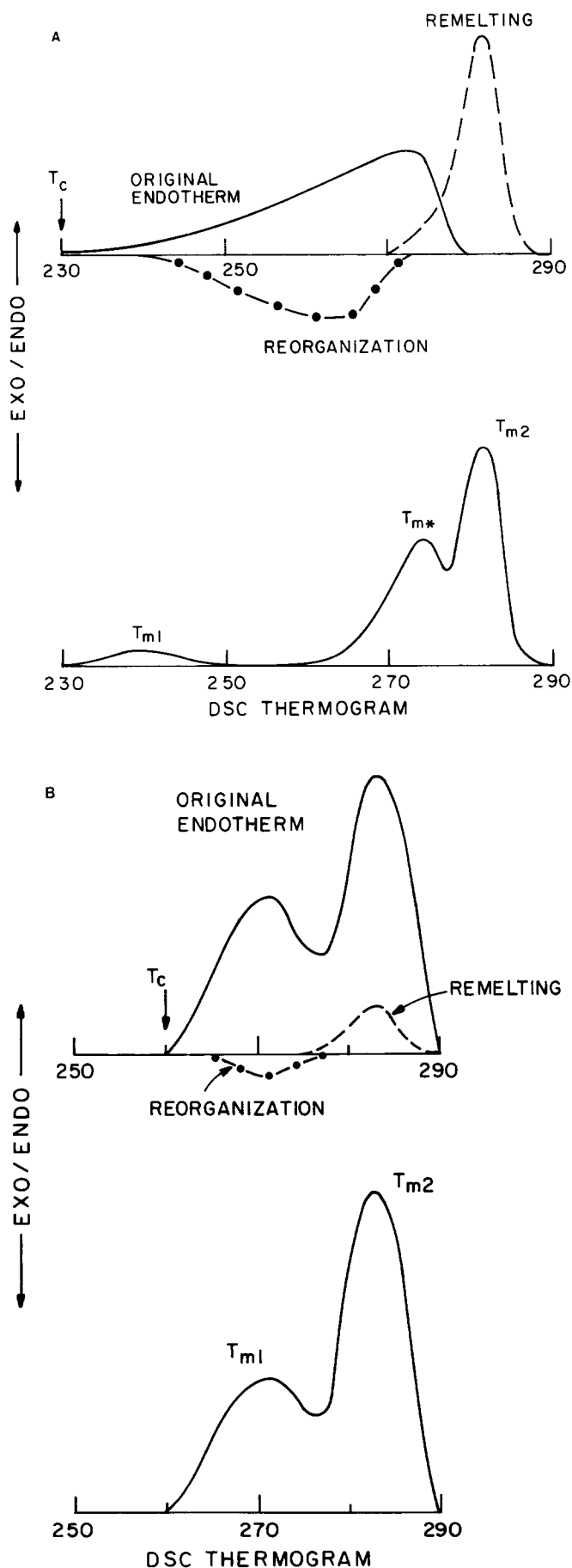


Figure 10 Proposed endothermic response of PPS crystallized: (A) at high undercooling; and (B) at low undercooling, showing original endotherm, reorganization and remelting endotherms, and resultant d.s.c. thermogram

at the crystallization temperature. Reorganization plays a minimal role in determining the appearance of the resultant d.s.c. endothermic response. If the crystallization takes place in the morphology dominated region, the upper melting peak temperature T_{m2} linearly increases as the crystallization temperature increases.

If PPS is melt crystallized at large undercooling, the crystals formed are relatively imperfect, forming quickly by rapid nucleation from a state of low mobility. There will be a broad distribution in crystal perfection, and crystals will be subject to reorganization during the d.s.c. scan. The multiple melting behaviour observed from this crystallization condition will have a large contribution from reorganization. The crystal structure and morphology are in the reorganization domain, and the dual melting endotherms found from the d.s.c. scan are then due to melting of the imperfect crystals, followed by reorganization and then remelting. In this case, it may be impossible to determine the true melting point of the room temperature population of crystals. When crystallization takes place in the reorganization domain, the upper melting peak temperature T_{m2} remains constant and is no longer a function of the crystallization temperature. The transition from morphology domination to reorganization occurs at roughly the same bulk crystallization rate for both grades of PPS used in this study.

ACKNOWLEDGEMENTS

The authors thank the Esther and Harold E. Edgerton Fund for support for this research, and Justyna Bodziuch for performing the scan rate studies. JSC acknowledges IBM for a predoctoral fellowship.

REFERENCES

- 1 Mills, P. J. and Hay, J. N. *Polymer* 1984, **25**, 1277
- 2 Zerbi, G., Piazza, R. and Holland-Moritz, K. *Polymer* 1982, **23**, 1921
- 3 Russel, T. P. *J. Polym. Sci., Polym. Phys. Edn.* 1985, **23**, 1109
- 4 Bell, T. P. and Dumbleton, J. H. *J. Polym. Sci. A-2* 1969, **7**, 1033
- 5 Bell, J. P., Slade, P. E. and Dumbleton, J. H. *J. Polym. Sci. A-2* 1968, **6**, 1773
- 6 Bell, J. P. and Murayama, T. *J. Polym. Sci. A-2* 1969, **7**, 1059
- 7 Mitomo, H. and Nakazato, K. *Polymer* 1978, **19**, 1427
- 8 Mitomo, H. *Polymer* 1988, **2**, 1635
- 9 Sweet, G. E. and Bell, J. P. *J. Polym. Sci. A-2* 1972, **10**, 1273
- 10 Nealy, D. L., Davis, T. G. and Kibler, C. J. *J. Polym. Sci. A-2* 1970, **8**, 2141
- 11 Roberts, R. C. *J. Polym. Sci. B* 1970, **8**, 381
- 12 Busfield, W. K. and Blade, C. S. *Polymer* 1980, **21**, 35
- 13 Wlochowicz, A. and Eder, M. *Polymer* 1984, **25**, 1268
- 14 Ghijssels, A., Groesbeek, N. and Yip, C. W. *Polymer* 1982, **23**, 1913
- 15 Sakaguchi, M. and Kashiwabara, H. *Polymer* 1982, **23**, 1594
- 16 Blundell, D. J. and Osborn, B. N. *Polymer* 1983, **24**, 953
- 17 Cebe, P. and Hong, S.-D. *Polymer* 1986, **27**, 1183
- 18 Cebe, P. *J. Mater. Sci.* 1988, **23**, 3721
- 19 Blundell, D. J. *Polymer* 1987, **28**, 2248
- 20 Lee, Y. and Porter, R. S. *Macromolecules* 1988, **21**, 2770
- 21 Lee, Y. and Porter, R. S. *Macromolecules* 1987, **20**, 1336
- 22 Cheng, S. Z. D., Cao, M.-Y. and Wunderlich, B. *Macromolecules* 1986, **19**, 1868
- 23 Nguyen, H. X. and Ishida, H. *Polymer* 1986, **27**, 1400
- 24 Sham, C. K., Guerra, G., Karasz, F. E. and Macknight, W. J. *Polymer* 1988, **29**, 1016
- 25 Bassett, D. C., Olley, R. H. and Al Raheil, I. A. M. *Polymer* 1988, **29**, 1745
- 26 Castles, J. L., Vallance, M. A., McKenna, J. M. and Cooper, S. Z. *J. Polym. Sci., Polym. Phys. Edn.* 1985, **23**, 2119

Melting behaviour of poly(phenylene sulphide). 1: J. S. Chung and P. Cebe

- 27 Leung, L. M. and Koberstein, J. T. *Macromolecules* 1986, **19**, 706
28 Stevenson, J. C. and Cooper, S. L. *Macromolecules* 1988, **21**, 1309
29 Turner-Jones, A. *Makromol. Chem.* 1971, **71**, 249
30 Bair, H. E. and Salovey, R. *J. Polym. Sci., Polym. Lett. Edn.* 1987, **5**, 429
31 Illers, K. H. and Hendus, H. *Makromol. Chem.* 1968, **113**, 1
32 Takamizawa, K., Fukahori, Y. and Urabe, Y. *Makromol. Chem.* 1969, **128**, 236
33 Wunderlich, B. 'Macromolecular Physics, Volume 3, Crystal Melting', Academic, New York, 1980, Ch. 9
34 Hellmuth, E. and Wunderlich, B. *J. Appl. Phys.* 1965, **36**, 3039
35 Jaffe, M. and Wunderlich, B. *Kolloid Z. Z. Polym.* 1967, **216**, 203
36 Starkweather, H. W. *J. Polym. Sci., Polym. Phys. Edn.* 1985, **23**, 1177
37 Bassett, D. C., Hodge, A. M. and Olley, R. H. *Dis. Faraday Soc.* 1979, **68**, 218
38 Bassett, D. C. and Hodge, A. M. *Proc. Roy. Soc.* 1978, **359**, 121
39 Cebe, P. and Chung, S. *Polym. Comp.* 1990, **11**, 265
40 Chung, J. S. and Cebe, P. *Polymer* 1992, **33**, 2325
41 Chung, J. S. and Cebe, P. *J. Polym. Sci., Polym. Phys. Edn* 1992, **30**, 163
42 Lovinger, A. J., Davis, D. D. and Padden, F. J. *Polymer* 1985, **26**, 1595
43 Lopez, L. C. and Wilkes, G. L. *Polymer* 1988, **29**, 106
44 Lopez, L. C., Wilkes, G. L. and Geibel, J. F. *Polymer* 1989, **30**, 147
45 Jog, J. P. and Nadkarni, V. M. *J. Appl. Polym. Sci.* 1985, **30**, 997
46 Hoffman, J. D. *Polymer* 1983, **24**, 3
47 Chung, S. and Cebe, P. *Polym. Preprints* 1990, **31**, 253
48 Cheng, S. Z. D., Wu, Z. Q. and Wunderlich, B. *Macromolecules* 1987, **20**, 2802
49 Calleja, F. S., Ortega, J. C. and De Salazar, I. M. *Polymer* 1978, **19**, 1094
50 Kitamaru, R. and Mandelkern, I. *J. Polym. Sci. A-2* 1970, **8**, 2079
51 Galvert, P. O. and Ryan, T. G. *Polymer* 1978, **19**, 611
52 Alfonso, G. C., Pedemonte, E. and Ponzetti, L. *Polymer* 1979, **20**, 104
53 Hay, J. N., Langford, J. I. and Lloyd, J. R. *Polymer* 1989, **30**, 489
54 Wakelyn, N. T. *J. Polym. Sci. Part C: Polym. Lett.* 1987, **25**, 25
55 Chung, J. S., Bodziuch, J. and Cebe, P. *J. Mater. Sci.* in press
56 Nichols, M. E. and Robertson, R. E. *Bull. Am. Phys. Soc.* 1991, **36**, 681